Hindawi
Journal of Chemistry
Volume 2018, Article ID 3547942, 10 pages
https://doi.org/10.1155/2018/3547942

Research Article

Synthesis and Evaluation of *N*-[1-(((3,4-Diphenylthiazol-2(3*H*)-ylidene)amino)methyl)cyclopentyl]acetamide Derivatives for the Treatment of Diseases Belonging to MAOs

Gülhan Turan-Zitouni,[1] **Aouatef Tabbi**,[1,2] **Weiam Hussein**,[1,3] **Abdullah Burak Karaduman**,[4] **Begüm Nurpelin Sağlık**,[1,5] **and Yusuf Özkay**[1,5]

[1]*Department of Pharmaceutical Chemistry, Faculty of Pharmacy, Anadolu University, 26470 Eskişehir, Turkey*
[2]*Department of Chemistry, Faculty of Sciences, Mentouri University, 325 Constantine, Algeria*
[3]*Department of Pharmaceutical Chemistry, Faculty of Pharmacy, Aden University, 6075 Aden, Yemen*
[4]*Department of Pharmaceutical Toxicology, Faculty of Pharmacy, Anadolu University, 26470 Eskişehir, Turkey*
[5]*Doping and Narcotic Compounds Analysis Laboratory, Faculty of Pharmacy, Anadolu University, 26470 Eskişehir, Turkey*

Correspondence should be addressed to Gülhan Turan-Zitouni; gturan@anadolu.edu.tr

Received 30 January 2018; Revised 18 March 2018; Accepted 13 August 2018; Published 13 September 2018

Academic Editor: Joaquin Campos

A series of *N*-[1-(((3,4-diphenylthiazol-2(3*H*)-ylidene)amino)methyl)cyclopentyl]acetamide derivatives (**4a-4i**) were synthesized in good yield and assayed for their inhibitory potency against monoamine oxidase (MAO) isoforms. Structures of newly synthesized compounds were characterized by IR, ^{1}H-NMR, ^{13}C-NMR, and mass spectroscopic methods. The inhibitory activity of compounds (**4a-4i**) against *h*MAO-A and *h*MAO-B enzymes was elucidated by using *in vitro* fluorometric method using Amplex Red® reagent. In the *h*MAO-A inhibition assay, compounds **4a**, **4b**, **4c**, and **4i** exhibited similar activity with standard drug moclobemide ($IC_{50} = 6.061 \pm 0.262\,\mu M$) with IC_{50} values of $7.06 \pm 0.18\,\mu M$, $6.56 \pm 0.20\,\mu M$, $6.78 \pm 0.15\,\mu M$, and $7.09 \pm 0.17\,\mu M$, respectively. According to *h*MAO-B inhibition results, compounds **4a**, **4b**, and **4c** displayed significant activity with IC_{50} values of $0.42 \pm 0.012\,\mu M$, $0.36 \pm 0.014\,\mu M$, and $0.69 \pm 0.020\,\mu M$, respectively. In the wake of all these results, it was understood that compound **4b** was found to be the most potent derivative in the series against both isoforms and selective as MAO-B inhibitor. The cytotoxicity test was performed for compounds **4a**, **4b**, and **4c**, and it was found that these compounds were noncytotoxic at the concentration of their IC_{50} values. Also, enzyme kinetic and docking studies of compound **4b** were performed against MAO-B. It was observed that **4b** showed a reversible and noncompetitive inhibition type. The important binding modes of this compound with active site of *h*MAO-B were shown owing to *in silico* studies.

1. Introduction

The frequency of Parkinson's disease (PD) is the most minimal in China, Japan, and Africa. In any case, it is emerging all through the world, in spite of stamped contrasts in demography, atmosphere, diet, sociocultural foundation, and industrialization [1]. In early stages of PD, there seems to be a compensatory increment in the quantity of dopamine receptors to suit the underlying loss of dopamine neurons. As the disease raise, number of dopamine receptors diminishes clearly because of the attending degeneration of dopamine in striatal neurons. The loss of dopaminergic neurons in PD [2] results in enhanced metabolism of dopamine, enlarging the arrangement of H_2O_2 and thus leading to generation of highly neurotoxic hydroxyl radicals (OH) [3]. The free radicals can also be produced by 6-hydroxydopamine or MPTP, which breaks down striatal dopaminergic neurons and causes Parkinsonism in experimental animals as well as human beings [4].

Monoamine oxidase (MAO) enzymes have two isoforms such as MAO-A and MAO-B, which share around 70% amino acids arrangement homology, and however vary in

their cell localization, substrate preference, and inhibitor affectability [5, 6]. Enzyme classes have critical parts in mental health. They manage the neurotransmitter capacity by metabolism in the brain, and by this way, they keep up proper concentration of intracellular amines [7]. In any case, overactivation of MAOs leads to production of neurotoxic by-products coming from neuronal variations. This biochemical event may result in disorders such as stroke, PD, and Alzheimer's disease (AD) [8, 9]. In the same way, modifications in other neurotransmitter frameworks are thought to be responsible for the behavioral unsettling influences [10].

Thiazole derivatives have potential against neurodiseases in the new drug development studies [11]. Furthermore, thiazole derivatives additionally can cross the blood-brain barrier [12]. In addition to thiazoles, acetamide derivatives are already known for their stimulatory effect on the central nervous system [13]. In the light of previously stated information and as a supplement of our researches on the same topic, we report herein the synthesis of some *N*-[1-(((3,4-diphenylthiazol-2(3*H*)-ylidene)amino)methyl)cyclopentyl]acetamide derivatives in order to investigate their ability to inhibit MAO enzymes.

2. Experimental

2.1. Chemistry. All chemicals were purchased from commercial supplier and used without purification. Melting points (mp) were determined on an Electrothermal 9100 melting point apparatus (Weiss-Gallenkamp, Loughborough, UK) and are uncorrected. IR spectra were recorded on Shimadzu 8400S spectrophotometer (Shimadzu, Tokyo, Japan), ^{1}H-NMR and ^{13}C-NMR spectra of the synthesized compounds were recorded on a Bruker 500 MHz spectrometer in DMSO d_6 using TMS as internal standard, and mass spectra were recorded on a LC/MS/MS Mass Spectrometer (3200 QTRAP, AB Sciex Instruments). Purity of synthesized compounds (**4a-4i**) was checked by Shimadzu LC-20A prominence HPLC system (Shimadzu, Tokyo, Japan), using acetonitrile (95%) and water (5%) mixture as a mobile phase at a flow rate of 0.8 ml/min.

*2.1.1. General Procedure for the Synthesis of the Intermediate Compounds (**1**, **2**, **3**).* *N*-(1-cyanocyclopentyl)acetamide (**1**) was synthesized via the method of Reihlen, Hessling, Hühn, and Weinbrenner [14]. The reduction of nitriles (**1**) gives *N*-[(1-aminomethyl)cyclopentyl]acetamide (**2**) by nickel Raney. A mixture of amine (**2**) (0.1 mol) and phenylisothiocyanate (0.1 mol) was refluxed in ethanol for 2 h. *N*-[(1-((3-phenylthioureido)methyl)cyclopentyl]acetamide (**3**) was filtered, washed with water, and dried. The product was crystallized from ethanol.

*2.1.2. N-[(1-((3-Phenylthioureido) methyl)cyclopentyl]acetamide (**3**).* Yield: 87%, Mp 230°C. IR νmax (cm^{-1}): 3470.70, 3375.20 (N–H stretching), 3260 (N–H stretching of acetamide), 1680 (C=O stretching of acetamide), 1560.95, 1510.32, 1467.46 (C=N and C=C stretching), 1210.17, 1168.00, 1095.45, 1010.01 (C–N stretching and aromatic C–H bending).

*2.1.3. General Procedure for Compounds (**4a-4i**).* *N*-[(1-((3-phenylthioureido)methyl)cyclopentyl]acetamide (**3**) (0.001 mol) and appropriate 2-bromo acetophenone derivative (0.001 mol) were refluxed in ethanol (20 mL) for 4 h. The reaction mixture was cooled and filtered.

*2.1.4. N-[1-(((3-Phenyl-4-(p-tolyl)thiazol-2(3H)-ylidene)amino) methyl)cyclopentyl]acetamide (**4a**).* ^{1}H-NMR (500 MHz, DMSO-d_6) d (ppm): 0.78–0.81 (2H, m, CH_2), 1.35–1.38 (2H, m, CH_2), 1.60–1.62 (2H, m, CH_2), 1.68 (3H, s, CH_3), 1.78 (3H, s, CH_3), 2.24–2.28 (2H, m, CH_2), 4.06 (2H, s, CH_2–N), 5.83 (1H, s, NH), 7.10–7.41 (9H, m, Ar–H), 8.71 (1H, s, thiazol-H). ^{13}C-NMR (125 MHz, DMSO-d_6, ppm): 22.83 (CH_2–CH_2), 21.25 (CH_3), 23.90 ($COCH_3$), 34.52 (2 CH_2), 47.63 (CH_2–NH), 65.42 (C), 98.27 (CH-thiazol), 120.40 (Ar-CH) 121.42 (Ar-2CH), 126.18 (Ar–C), 128.07 (Ar-2CH), 129.12 (Ar-2CH), 130.07 (Ar-2CH), 133.05 (Ar–C), 136.62 (Ar–C), 138.55 (Ar–C), 140.30 (Ar–C), 149.34 (thiazol-C), 159.15 (N=C-thiazol), 170.12 (CO). MS [M + 1]+: m/z 406 (100%). HPLC: 99.4% purity.

*2.1.5. N-[1-(((4-(4-Methoxyphenyl)-3-phenylthiazol-2(3H)-ylidene)amino)methyl)cyclopentyl]acetamide (**4b**).* ^{1}H-NMR (500 MHz, DMSO-d_6) d (ppm): 0.78–0.80 (2H, m, CH_2), 1.34–1.37 (2H, m, CH_2), 1.56–1.62 (2H, m, CH_2), 1.79 (3H, s, CH_3), 2.26–2.32 (2H, m, CH_2), 3.88 (3H, s, OCH_3), 4.07 (2H, s, CH_2–N), 5.79 (1H, s, NH), 7.00 (2H, d J = 8.60 Hz, Ar–H), 7.11–7.13 (3H, m, Ar–H), 7.30 (2H, d J = 8.70, Ar–H), 7.38–7.41 (2H, m, Ar–H), 8.90 (1H, s, thiazol-H). ^{13}C-NMR (125 MHz, DMSO-d_6, ppm): 22.82 (CH_2–CH_2), 23.95 ($COCH_3$), 34.61 (2 CH_2), 48.63 (CH_2–NH), 55.69 (O–CH_3), 65.67 (C), 96.17 (CH-thiazol), 114.48 (Ar-2CH), 121.39 (Ar-2CH), 123.11 (Ar-2CH), 129.10 (Ar-CH), 130.02 (Ar-2CH), 130.07 (Ar-2CH), 133.05 (Ar–C), 133.69 (Ar–C), 139.57 (Ar–C), 151.61 (thiazol-C), 161.16 (N=C-thiazol), 169.18 (CO). MS [M + 1]+: m/z 422 (100%). HPLC: 98.6% purity.

*2.1.6. N-[1-(((4-(4-Nitrophenyl)-3-phenylthiazol-2(3H)-ylidene)amino)methyl)cyclopentyl]acetamide (**4c**).* ^{1}H-NMR (500 MHz, DMSO-d_6) d (ppm): 0.96 (2H, br, CH_2), 1.48 (2H, br, CH_2), 1.61 (2H, br, CH_2), 1.76 (3H, s, CH_3), 2.21 (2H, br, CH_2), 4.22 (2H, br, CH_2–N), 5.98 (1H, br, NH), 7.15 (3H, m, Ar–H), 7.41 (2H, d J = 8.2 Hz, Ar–H), 7.60 (2H, d J = 8.1 Hz, Ar–H), 7.78 (1H, br, thiazol-H), 8.37 (2H, d J = 7.35 Hz, Ar–H). ^{13}C-NMR (125 MHz, DMSO-d_6, ppm): 22.66 (CH_2–CH_2), 23.63 ($COCH_3$), 35.09 (2 CH_2), 48.27 (CH_2–NH), 65.67 (C), 100.40 (CH-thiazol), 121.19 (Ar-2CH), 123.46 (Ar–C), 124.28 (Ar-2CH), 129.83 (Ar-2CH), 130.12 (Ar-2CH), 138.59 (Ar–C), 138.90 (Ar–C), 147.33 (thiazol-C), 151.46 (Ar–C), 161.17 (N=C-thiazol), 169.67 (CO). MS [M + 1]+: m/z 437 (100 %). HPLC: 99.2% purity.

*2.1.7. N-[1-(((4-(4-Fluorophenyl)-3-phenylthiazol-2(3H)-ylidene)amino)methyl)cyclopentyl]acetamide (**4d**).* ^{1}H-NMR (500 MHz, DMSO-d_6) d (ppm): 0.79–0.80 (2H, m, CH_2), 1.34–1.39 (2H, m, CH_2), 1.59–1.62 (2H, m, CH_2), 1.78 (3H, s, CH_3), 2.24–2.29 (2H, m, CH_2), 4.07 (2H, s, CH_2–N), 5.83 (1H, s, NH), 7.11–7.13 (3H, m, Ar–H), 7.18 (2H, t, Ar–H), 7.36–7.42 (4H, m, Ar–H), 8.72 (1H, s, thiazol-H). ^{13}C-NMR (125 MHz, DMSO-d_6, ppm): 22.76 (CH_2–CH_2), 23.88 ($COCH_3$), 34.80 (2 CH_2), 48.40 (CH_2–NH), 65.61 (C), 97.21 (CH-thiazol), 115.88 (Ar-CH), 116.17 (Ar-CH), 121.31 (Ar-2CH), 123.18 (Ar–C), 128.73 (Ar–C), 128.77 (Ar-2CH), 129.10 (Ar-CH), 131.45 (Ar-2CH), 139.70 (Ar–C), 151.61 (thiazol-C), 161.20 (Ar–C), 164.17 (N=C-thiazol), 169.18 (CO). MS [M + 1]+: m/z 410 (100 %). HPLC: 98.7% purity.

*2.1.8. N-[1-(((4-(4-Chlorophenyl)-3-phenylthiazol-2(3H)-ylidene)amino)methyl)cyclopentyl]acetamide (**4e**).* ^{1}H-NMR (500 MHz, DMSO-d_6) d (ppm): 0.83–0.85(2H, m, CH_2), 1.35–1.39 (2H, m, CH_2), 1.60–1.64 (2H, m, CH_2), 1.78 (3H, s, CH_3), 2.24–2.28 (2H, m, CH_2), 4.09 (2H, s, CH_2–N), 5.84 (1H, s, NH), 7.11–7.14 (3H, m, Ar–H), 7.28 (2H, d J = 8.40, Ar–H), 7.38 (2H, t, Ar–H), 7.46 (2H, d J = 8.35 Hz, Ar–H), 8.54 (1H, s, thiazol-H). ^{13}C-NMR (125 MHz, DMSO-d_6, ppm): 22.75 (CH_2–CH_2), 23.77 ($COCH_3$), 34.89 (2 CH_2), 48.33 (CH_2–NH), 65.68 (C), 97.77 (CH-thiazol), 121.28 (Ar-2CH), 123.21 (Ar-2CH), 129.10 (Ar-CH), 130.02 (Ar-2CH), 130.07 (Ar-Ar-(Ar-2CH), 124.57 (Ar–C), 129.98 (Ar-2CH), 130.75 (Ar-CH), 140.59 (Ar–C), 151.66 (thiazol-C), 159.86 (Ar–C), 161.41 (N=C-thiazol), 169.07 (CO). MS [M + 1]+: m/z 426 (100 %). HPLC: 99.5% purity.

*2.1.9. N-[1-(((4-(4-Bromophenyl)-3-phenylthiazol-2(3H)-ylidene)amino)methyl)cyclopentyl]acetamide (**4f**).* ^{1}H-NMR (500 MHz, DMSO-d_6) d (ppm): 0.85–0.90 (2H, m, CH_2), 1.37–1.39 (2H, m, CH_2, 1.59–1.63 (2H, m, CH_2), 1.78 (3H, s, CH_3), 2.26–2.28 (2H, m, CH_2), 4.09 (2H, s, CH_2–N), 5.84 (1H, s, NH), 7.10–7.15 (3H, m, Ar–H), 7.25–7.28 (2H, d J = 8.40 Hz, Ar–H), 7.38–7.41 (2H, t, Ar–H), 7.62–7.64 (2H, d J = 8.40 Hz, Ar–H), 8.50 (1H, s, thiazol-H). ^{13}C-NMR (125 MHz, DMSO-d_6, ppm): 22.75 (CH_2–CH_2), 23.76 ($COCH_3$), 34.91 (2 CH_2), 48.32 (CH_2–NH), 65.57 (C), 97.75 (CH-thiazol), 121.28 (Ar-2CH), 122.34 (Ar–C), 123.21 (Ar–C), 130.03 (Ar-2CH), 131.09 (Ar-2CH), 131.51 (Ar–C), 132.02 (Ar-2CH), 139.62 (Ar–C), 151.61 (thiazol-C), 161.16 (N=C-thiazol), 169.18 (CO). MS [M + 1]+: m/z 470 (100 %). HPLC: 98.9% purity.

*2.1.10. N-[1-(((4-(3,4-Dichlorophenyl)-3-phenylthiazol-2(3H)-ylidene)amino)methyl)cyclopentyl]acetamide (**4g**).* ^{1}H-NMR (500 MHz, DMSO-d_6) d (ppm): 0.96–0.97 (2H, m, CH_2), 1.42–1.44 (2H, m, CH_2), 1.61–1.66 (2H, m, CH_2), 1.76 (3H, s, CH_3), 2.24–2.27 (2H, m, CH_2), 4.11 (2H, s, CH_2–N), 5.86 (1H, s, NH), 7.09–7.14 (3H, m, Ar–H), 7.22 (1H, d, Ar–H), 7.38–7.41 (2H, t, Ar–H), 7.51–7.515 (1H, d J = 2.0 Hz, Ar–H), 7.57–7.58 (1H, d J = 8.25 Hz, Ar–H), 8.19 (1H, d, thiazol-H). ^{13}C-NMR (125 MHz, DMSO-d_6, ppm): 22.75 (CH_2–CH_2), 23.62 ($COCH_3$), 35.09 (2 CH_2), 48.27 (CH_2–NH), 65.63 (C), 98.75 (CH-thiazol), 121.20 (Ar-2CH), 123.27 (Ar-CH), 129.09 (Ar-CH), 130.07 (Ar–C), 130.87 (Ar-2CH), 131.11 (Ar–C), 131.56 (Ar–C), 131.82 (Ar-CH), 132.80 (Ar–C), 138.35 (Ar–C), 57 (Ar–C), 151.55 (thiazol-C), 160.96 (N=C-thiazol), 169.14 (CO). MS [M + 1]+: m/z 460 (100 %). HPLC: 98.4% purity.

*2.1.11. N-[1-(((4-(2-Hydroxy-5-methoxyphenyl)-3-phenylthiazol-2(3H)-ylidene)amino)methyl) cyclopentyl]acetamide (**4h**).* ^{1}H-NMR (500 MHz, DMSO-d_6) d (ppm): 1.06 (2H, br, CH_2), 1.28 (2H, br, CH_2), 1.62 (2H, br, CH_2), 1.86 (3H, s, CH_3), 2.30 (2H, br, CH_2), 3.79 (2H, s, CH_2–N), 3.85 and 3.88 (2H, d s, OCH_3), 5.77 and 5.88 (1H, d s, NH), 6.53–6.59 (2H, m, Ar–H), 7.07–7.15 (4H, t, Ar–H), 7.37–7.40 (2H, t, Ar–H), 7.98 (1H, s, thiazol-H). ^{13}C-NMR (125 MHz, DMSO-d_6, ppm): 22.70 (CH_2–CH_2), 23.74 ($COCH_3$), 36.08 (2 CH_2), 48.07 (CH_2–N), 56.03 (OCH_3), 64.07 (C), 100.02 (CH-thiazol) 111.70 (Ar-CH), 114.02 (Ar-CH), 119.03 (Ar-CH), 121.95 (Ar-CH), 122.80 (Ar-2CH), 130.02 (Ar-2CH), 140.87 (Ar–C), 146.11 (thiazol-C), 149.92 (Ar-C-OH), 152.50 (Ar-C-OCH_3), 158.55 (N=C-thiazol), 170.14 (CO). MS [M + 1]+: m/z 437 (100 %). HPLC: 99.6% purity.

*2.1.12. N-[1-(((4-(3-Nitrophenyl)-3-phenylthiazol-2(3H)-ylidene)amino)methyl)cyclopentyl]acetamide (**4i**).* ^{1}H-NMR (500 MHz, DMSO-d_6) d (ppm): 1.02 (2H, br, CH_2), 1.27 (2H, br, CH_2), 1.59 (2H, br, CH_2), 1.81 (3H, s, CH_3), 2.25 (2H, br, CH_2), 4.29 (2H, s, CH–N), 6.1 (1H, s, NH), 7.28 (1H, s, Ar–H), 7.43–7.45 (3H, t, Ar–H), 7.74–7.78 (4H, m, Ar–H), 8.32 (1H, s, thiazol-H), 8.37 (1H, d, Ar–H). ^{13}C-NMR (125 MHz, DMSO-d_6, ppm): 22.72 (CH_2–CH_2), 23.42 ($COCH_3$), 35.39 (2 CH_2), 49.21 (CH_2–NH), 65.61 (C), 99.85 (CH-thiazol), 120.02 (Ar-CH), 121.90 (Ar-CH), 123.00 (Ar-2CH), 123.01 (Ar-CH), 129.54 (Ar-2CH), 130.07 (Ar–C), 130.87 (Ar-CH), 134.11 (Ar-CH), 135.53 (Ar–C), 140.02 (Ar–C), 147.00 (Ar–C)), 151.55 (thiazol-C), 157.08 (N=C-thiazol), 160.96 (N=C-thiazol), 169.14 (CO). MS [M + 1]+: m/z 437 (100 %). HPLC: 99.7% purity.

2.2. MAO-A and MAO-B Inhibition Assay. MAO enzyme inhibition assay, based on fluorometric measurements, was used to determine the inhibition profiles of all synthesized compounds as previously defined by us [15, 16]. The reagents used in the enzymatic assay including Ampliflu™ Red (10-acetyl-3,7-dihydroxyphenoxazine), peroxidase from horseradish, *h*MAO-A, *h*MAO-B, H_2O_2, tyramine hydrochloride, selegiline, and moclobemide were purchased from Sigma-Aldrich (Steinheim, Germany). All dilution and pipetting processes were carried out by the robotic system, BioTek Precision XS (BioTek Instruments, Winooski, VT, USA). BioTek-Synergy H1 microplate reader was used to record the fluorescence measurements (excitation, 535 nm; emission, 587 nm) over a 30 min period, in which the fluorescence increased linearly.

2.3. Enzyme Kinetic Studies. In order to investigate the inhibition type of compound **4b** on *h*MAO-B, enzyme kinetic

study was applied according to the previous studies reported by us [15, 16].

2.4. Cytotoxicity Test. MTT test was performed to determine the cytotoxic profile of the most active compounds **4a**, **4b**, and **4c** using the NIH/3T3 mouse embryonic fibroblast cell line (ATCC® CRL-1658™, London, UK). The method was carried out in the same way as we have reported in our previous studies [15–18].

2.5. Molecular Docking Studies. A structure-based *in silico* procedure was applied to discover the binding modes of compound **4b** *h*MAO-B enzyme active site. The crystal structures of *h*MAO-B (PDB ID: 2V5Z) [19], which was crystallized with the reversible inhibitor safinamide, was retrieved from the Protein Data Bank server (http://www.pdb.org). The docking procedure was applied as previously described by our research group [16].

3. Result and Discussion

3.1. Chemistry. The synthesis of thiazoline derivatives (**4a-4i**) was carried out according to the steps shown in Scheme 1.

N-(1-cyanocyclopentyl)acetamide (**1**) was synthesized via the method of Reihlen, Hessling, Hühn, and Weinbrenner [14]. The reduction of nitriles (**1**) gives *N*-[(1-aminomethyl)cyclopentyl]acetamide (**2**) by nickel Raney [20]. Secondly, *N*-[(1-((3-phenylthioureido)methyl)cyclopentyl]acetamide (**3**) was synthesized via the reaction of compound **2** with phenyl isothiocyanates [21] (Scheme 1). The ring closure reaction of the intermediate compound (**3**) with phenacyl bromides afforded the title compounds (**4a-4i**) (Scheme 1 and Table 1). The structures of the compounds were confirmed by ^{1}H-NMR, ^{13}C-NMR, mass spectroscopy, and elemental analysis.

In the IR spectra of compounds **4a-4i**, C=N and C=C stretching vibrations were observed in the region 1645–1470 cm^{-1}. The aromatic C–H stretching vibrations gave rise to bands at 3120–3010 cm^{-1}.

In the ^{1}H-NMR spectra, the protons corresponding to cyclopentyl, resonated as multiplets at *d* 0.78–0.85 ppm, 1.34–1.40 ppm, 1.56–1.65 ppm, and 2.25–2.35 ppm, and CH_2–N protons appeared as singlet at *d* 4.09 ppm. The protons of acetamide appeared as a singlet at *d* 5.80 ppm. All the other aromatic and aliphatic protons were observed at expected regions.

^{13}C-NMR chemical shift values of the carbon atoms at 22.60–22.85 and 34.50–36.10 ppm (cyclopentyl CH_2), 23.60–23.90 ppm ($COCH_3$), 47.60–48.65 ppm (CH_2–NH), 159.10–161.45 ppm (N=C-thiazol), and 169.05–170.15 ppm (CO) corroborate the compounds deduced from the ^{1}H-NMR data. All the other aromatic carbon atoms were observed at expected areas.

The mass spectra of compounds (**4a-4i**) are also in agreement with their molecular formula. According to HPLC analysis, purity ratio was found between 98.4 and 99.7%. Peak purity index of all compounds was also checked, and no impurity was determined in observed peaks.

3.2. MAO-A and MAO-B Inhibition Assay. In order to investigate *h*MAO-A and *h*MAO-B inhibitory activity of all end compounds (**4a-4i**), an *in vitro* fluorometric method, which is on the strength of the detection of H_2O_2 in a horseradish peroxidase-coupled reaction using Amplex Red reagent, was used. The activity results against both isoenzymes by using all compounds at the concentration of 10^{-3} and 10^{-4} M were obtained as a result of second stage of the activity tests. In this second step, compounds showing more than 50% inhibition in the first step were selected and their further concentrations (10^{-5}–10^{-9} M) were studied. Also, IC_{50} graphs, obtained from GraphPad "Prism" software (version 5.0), of these selected compounds can be observed in Figures 1 and 2.

All compounds except for compound **4h** showed high percent inhibition against *h*MAO-A in the first step of activity studies. Among these compounds, **4a**, **4b**, **4c**, and **4i** exhibited similar activity with standard drug moclobemide ($IC_{50} = 6.061 \pm 0.262\,\mu$M) with IC_{50} values of $7.06 \pm 0.18\,\mu$M, $6.56 \pm 0.20\,\mu$M, $6.78 \pm 0.15\,\mu$M, and $7.09 \pm 0.17\,\mu$M, respectively. When analyzing *h*MAO-B activity results, none of the compounds except for compounds **4a**, **4b**, and **4c** displayed remarkable activity. These compounds, **4a**, **4b**, and **4c**, displayed *h*MAO-B inhibition profile with IC_{50} values of $0.42 \pm 0.012\,\mu$M, $0.36 \pm 0.014\,\mu$M, and $0.69 \pm 0.020\,\mu$M, respectively. According to all these results, it can be understood that compound **4b** is the most potent derivative against MAO-A and MAO-B isoenzymes. It can also be suggested that compound **4b** could be a selective MAO-B inhibitor when its IC_{50} values on these enzymes are considered.

3.3. Kinetic Studies of Enzyme Inhibition. The mechanism of *h*MAO-B inhibition was investigated by enzyme kinetics, following a similar procedure to the MAO inhibition assay. The linear Lineweaver–Burk graphics were used to estimate the type of inhibition. Enzyme kinetics were analyzed by recording substrate velocity curves in the absence and presence of the most potent compound **4b**, which was prepared at concentrations of $IC_{50}/2$, IC_{50}, and $2xIC_{50}$. In each case, the initial velocity measurements were gained at different substrate (tyramine) concentrations ranging from 20 μM to 0.625 μM. The K_i (intercept on the *x*-axis) values of compound **4b** were determined from the secondary plot of the K_m/V_{max} (slope) versus varying concentrations. The graphical analysis of steady-state inhibition data for compound **4b** is shown in Figure 3.

Based on the type of interaction with the enzyme, inhibitor binding can be classified as either reversible or irreversible. The type of inhibition can be determined by the Lineweaver–Burk plot as mixed type, uncompetitive, competitive, or noncompetitive, which are the indicators of a reversible inhibitor [22]. It is known that, in the uncompetitive type inhibition, a graphic, including the parallel lines without any cross, is observed. If the lines cross neither the *x*- nor the *y*-axis at the same point, the inhibition type is called mixed type. Competitive inhibitors possess the same intercept on the *y*-axis, but there are diverse slopes and

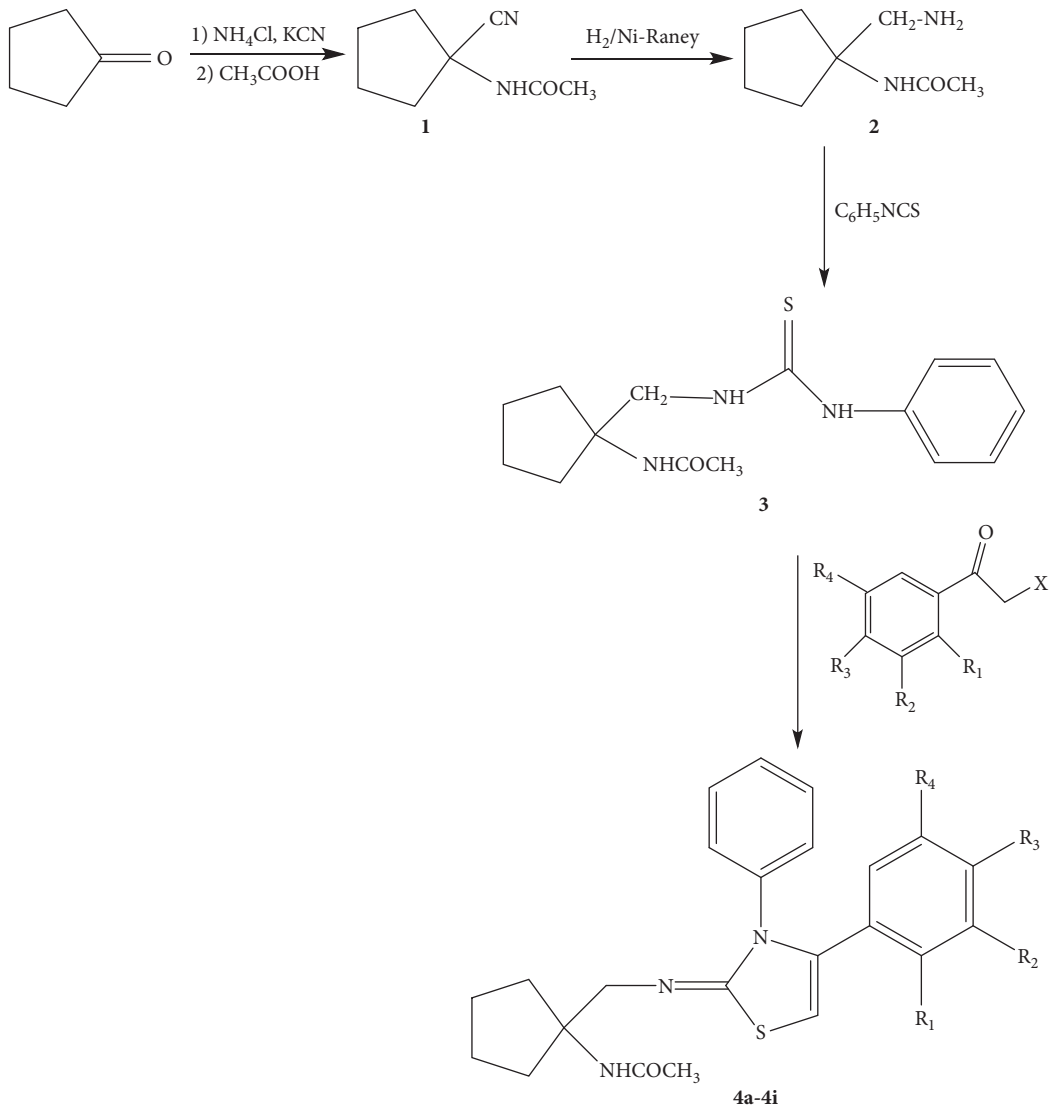

Scheme 1: Synthesis pathway of targeted compounds.

Table 1: Newly synthesized compounds (**4a-4i**).

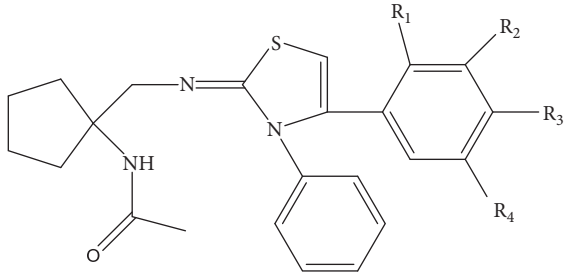

Compounds	R_1	R_2	R_3	R_4	MW
4a	H	H	CH_3	H	405.19
4b	H	H	OCH_3	H	421.18
4c	H	H	NO_2	H	436.16
4d	H	H	F	H	409.16
4e	H	H	Cl	H	425.13
4f	H	H	Br	H	469.08
4g	H	Cl	Cl	H	459.09
4h	OH	H	H	OCH_3	437.18
4i	H	NO_2	H	H	436.16

intercepts on the x-axis between the two datasets. On the other hand, noncompetitive inhibition has plots with the same intercept on the x-axis, but there are different slopes and intercepts on the y-axis, which is observed in Figure 3. Therefore, this pattern indicates that the compound **4b** is reversible and noncompetitive inhibitor and can bind to either the free enzyme or the enzyme-substrate complex. K_i value for compound **4b** was calculated as 0.346 μM for the inhibition of *h*MAO-B.

Reversible inhibitors bind to enzymes by noncovalent interactions as hydrophobic interactions, ionic bonds, and hydrogen bonds without forming any chemical bonds or reactions with the enzyme. These interactions are formed rapidly and can be easily removed; hence, the enzyme and inhibitor complex are quickly dissociated opposite to irreversible inhibition. Due to reversible binding ability to biomolecules, such inhibitors carry a lower risk of side effects compared to irreversible inhibitors. As a result, reversible-noncompetitive inhibition potency of compound **4b** has enhanced their biological importance.

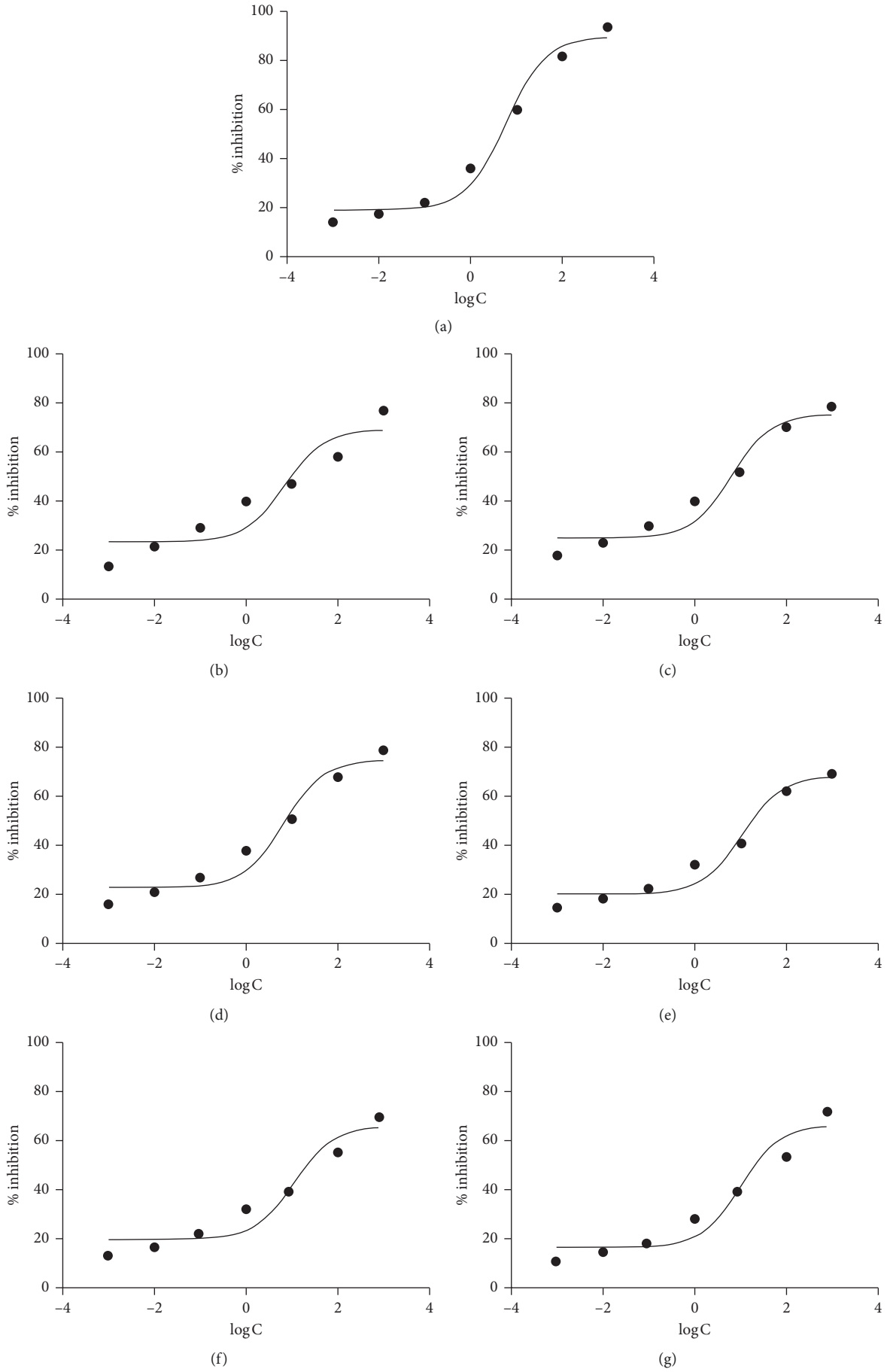

Figure 1: Continued.

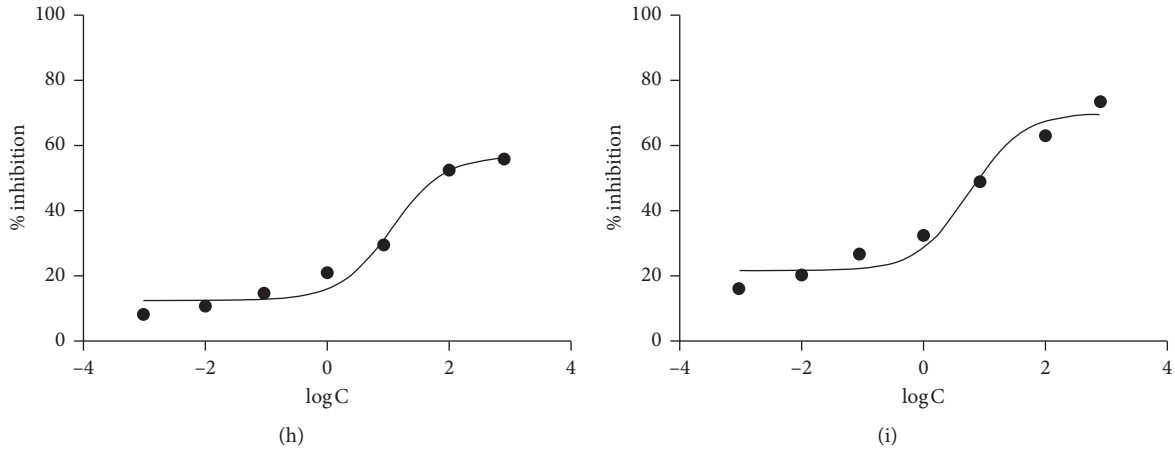

Figure 1: IC_{50} (μM) of the selected compounds (**4a**, **4b**, **4c**, **4d**, **4e**, **4f**, **4g**, and **4i**) and control drugs against MAO-A enzyme. (a) Moclobemide (6.06 μM); (b) 4a (7.06 μM); (c) 4b (6.56 μM); (d) 4c (6.78 μM); (e) 4d (10.98 μM); (f) 4e (13.08 μM); (g) 4f (12.41 μM); (h) 4g (13.45 μM); (i) 4i (7.09 μM).

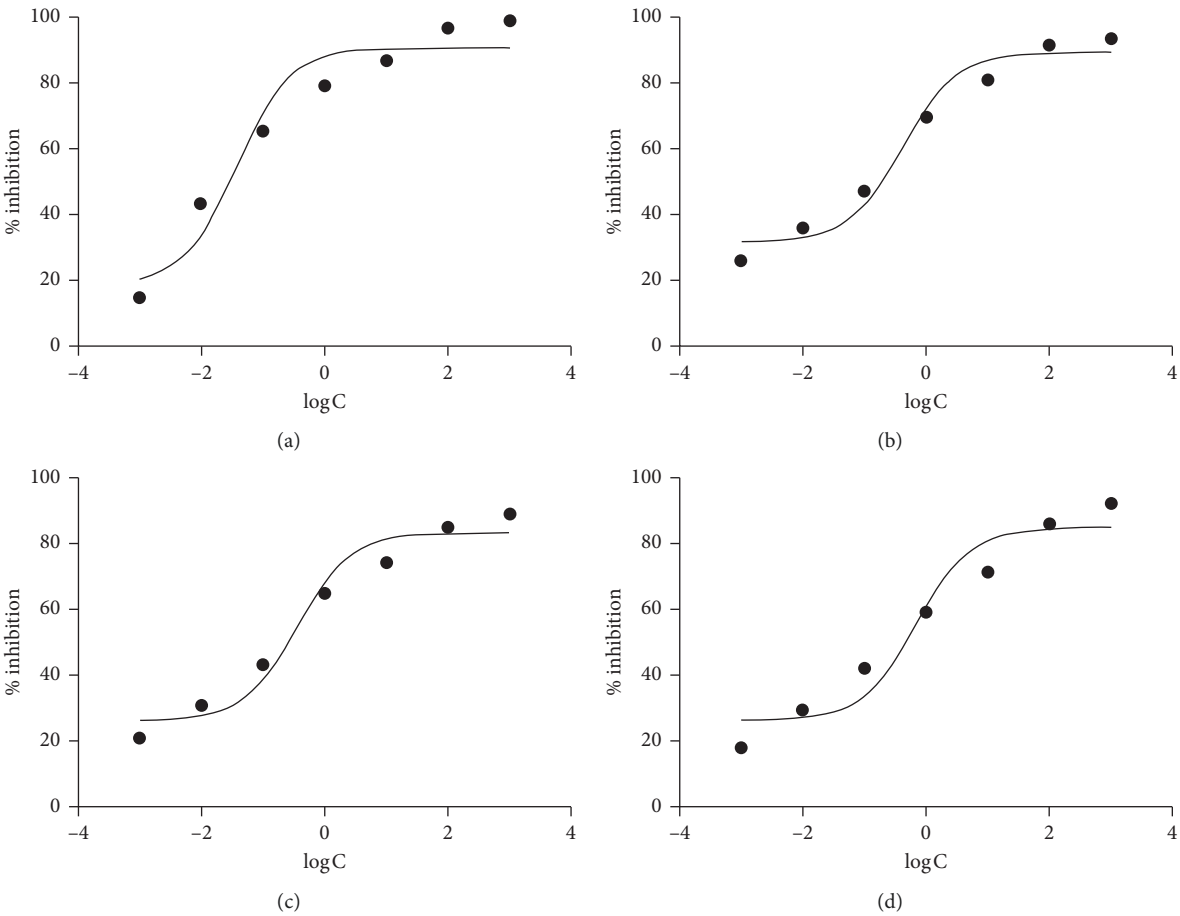

Figure 2: IC_{50} (μM) of the selected compounds (**4a**, **4b**, and **4c**) and control drugs against MAO-B enzyme. (a) Selegiline (0.038 μM); (b) 4a (0.42 μM); (c) 4b (0.36 μM); (d) 4c (0.69 μM).

3.4. Cytotoxicity Test. The cytotoxic activity of compounds **4a**, **4b**, and **4c** was evaluated against healthy NIH/3T3 mouse embryonic fibroblast cell line (ATCC CRL1658), which is suggested for preliminary cytotoxicity screening by ISO (10993-5, 2009) [23]. The IC_{50} values of the compounds are represented in Table 2. Compounds **4a**, **4b**, and **4c** displayed higher IC_{50} values against NIH/3T3 cells than their IC_{50} values (0.42, 0.36, and 0.69 μM, resp.) against *h*MAO-B. This result reveals that compounds **4a**, **4b**, and **4c** are not cytotoxic at their effective concentration against *h*MAO-B.

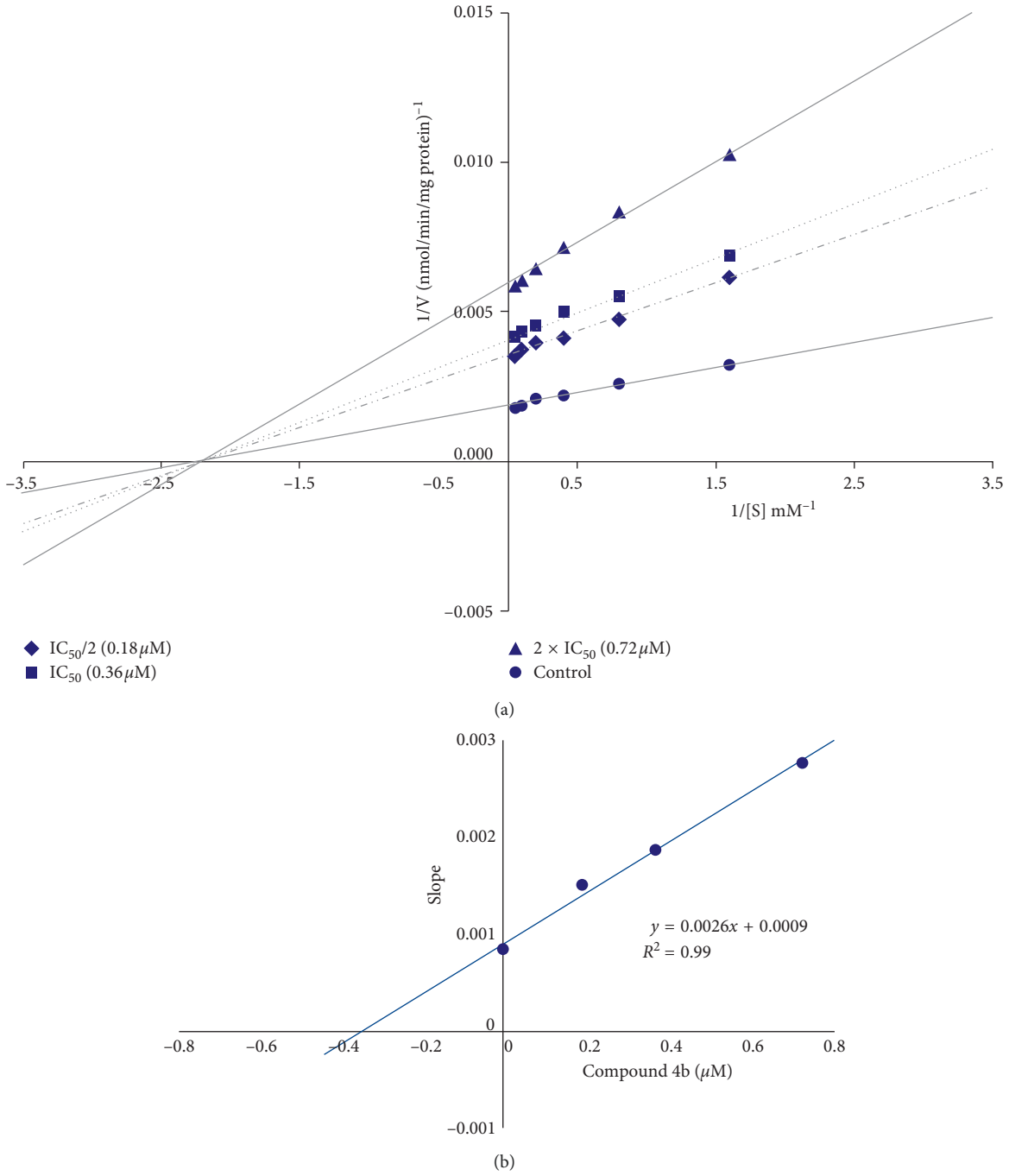

Figure 3: (a) Lineweaver–Burk plots for the inhibition of *h*MAO-B by compound **4b**. [S], substrate concentration (μM); V, reaction velocity (nmol/min/mg protein). Inhibitor concentrations are shown at the left. V_{max} values from 2xIC$_{50}$ to control: 172.565, 243.902, 277.778, and 525.120 (nmol/min/mg protein). K_m value of the noncompetitive inhibition: 0.443 ± 0.018 (μM). (b) Secondary plot for calculation of steady-state inhibition constant (K_i) of compound **4b**. K_i was calculated as 0.346 μM.

Table 2: Cytotoxic activity of compounds **4a**, **4b**, and **4c** against NIH/3T3 cell line.

Compound	IC50 (μM)
4a	>1000
4b	>1000
4c	>1000

3.5. Molecular Docking Studies. As stated in the MAO inhibition studies, compound **4b** was found to be the most active and selective derivative against *h*MAO-B isoform. In order to assess this *in vitro* activity and find out the binding modes of compound **4b**, docking studies were performed by using Maestro interface. X-ray crystal structure of *h*MAO-B, obtained from Protein Data Bank server (http://www.pdb.org),

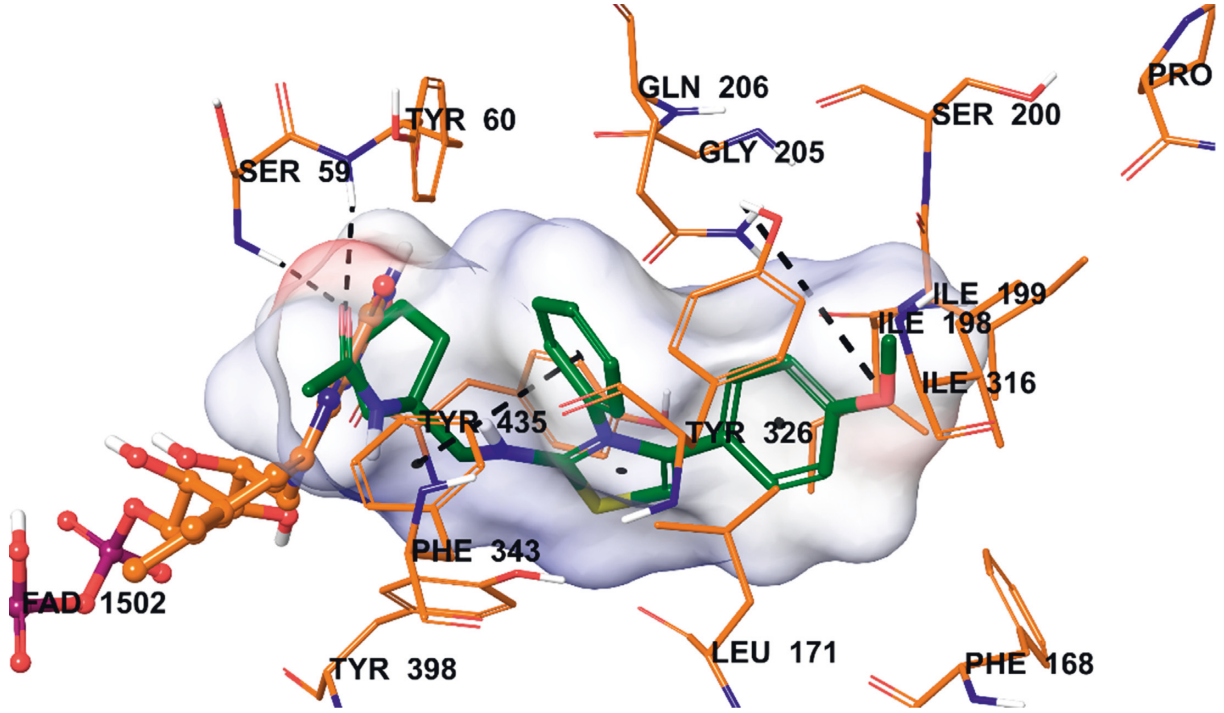

Figure 4: Docking studies including interacting modes of compound **4b** in the active region of *h*MAO-B. The inhibitor and the important residues in the active site of the enzyme are presented by tube model. The FAD molecule is colored orange with ball and stick model.

was used (PDB ID: 2V5Z) [19]. The docking pose of compound **4b** is presented in Figure 4.

It can be seen that compound **4b** is located in close proximity to the FAD cofactor and binds tightly to the amino acid residues in the cavity. According to the docking pose, compound **4b** interacts with the active site by establishing three hydrogen bonds and a *p*-π interaction. This *p*-π interaction is observed between the phenyl ring attached to the nitrogen atom of thiazole and phenyl of Phe343. Two of the other hydrogen bonds are associated with the amide carbonyl in the structure. This moiety creates these hydrogen bonds with amino groups of Ser59 and Tyr60. The last hydrogen bond is formed between the methoxy group, stated at the C-4 position of the phenyl ring, and hydroxyl of Tyr326. It is thought that this additional bond is very important in terms of enzyme activity.

When the chemical structures of the synthesized compounds are compared with each other, it is seen that varying substituents at the C-2, C-3, C-4, and C-5 positions of the phenyl ring is the main reason of structural difference. It is considered by analyzing especially the activity results on *h*MAO-B that the substituents at the C-4 position of the phenyl increase the activity and selectivity. Furthermore, according to the results obtained from docking studies, as in compound **4b**, functional groups such as methoxy moiety with the capacity to establish hydrogen bonds at this position bind more strongly to active region of enzyme and thus are important for activity. On the contrary, incorporation of both methoxy and hydroxyl groups in the C-2 and C-4 positions of phenyl ring as in the compound **4h** showed no activity. This might be referred to the steric hindrance in general which may increase as the distance between two substituents decreases [24].

4. Conclusion

Another class of *N*-[1-(((3-Phenyl-4-(p-tolyl)thiazol-2(3H)-ylidene)amino)methyl)cyclopentyl]acetamide derivatives (**4a-4i**), bearing active thiazole moiety which contributes to MAO inhibition, was designed and synthesized. According to activity results, compounds **4a**, **4b**, and **4c** showed good activity on both isoenzymes. Among the series, compound **4b** was found as most active derivative and selective MAO-B inhibitor. Furthermore, enzyme kinetic, toxicological, and docking evaluations of compound **4b** were undertaken in the current study. The type of inhibition of this compound was found as reversible and noncompetitive. In addition, this active compound was not cytotoxic at MAO inhibitors IC_{50} value given. Docking studies clearly indicated interactions between compound **4b** and *h*MAO-B. Consequently, the study gave significant data to further improvement and change of medications for the treatment of diseases connected with MAOs. The information of this study recommends these compounds as promising leads for the development of novel MAO inhibitors with a decent inhibitory power, which in turn may fill the gap in the curative weapons store for Parkinson's disease (PD) in particular.

Data Availability

The data used to support the findings of this study are available from the corresponding author upon request.

Conflicts of Interest

The authors declare that there are no conflicts of interest regarding the publication of this paper.

Acknowledgments

This study was financially supported by Anadolu University Scientific Projects Fund, Project no. 1805S189.

References

[1] Z. X. Zhang and G. C. Roman, "Worldwide occurrence of Parkinson's disease: An updated review," *Neuroepidemiology*, vol. 12, no. 4, pp. 195–208, 1993.

[2] O. Hornykiewicz and S. J. Kish, "Biochemical pathology of Parkinson's disease," *Advance in Neurology*, vol. 45, pp. 19–34, 1986.

[3] M. Naoi and W. Maruyama, "Type B monoamine oxidase and neurotoxins," *Europe Neurology*, vol. 33, no. 1, pp. 31–37, 1993.

[4] Y. Mitzuno, N. Sone, and T. Saitoh, "Effects of 1-methyl-4-phenyl- 1,2,3,6 tetrahydropyridine and I-methyl-4-phenylpyridinium ion on activities of the enzymes in the electron transport system in mouse brain," *Journal of Neurochemistry*, vol. 48, no. 6, pp. 1787–1793, 1987.

[5] C. Binda, P. F. Newton-Vinson, D. E. Hubálek et al., "Structure of human monoamine oxidase B, a drug target for the treatment of neurological disorders," *Nature Structural Biology*, vol. 9, no. 1, pp. 6–22, 2002.

[6] K. F. Tipton, S. Boyce, G. O. Sullivan et al., "Monoamine oxidases: certainties and uncertainties," *Current Medicinal Chemistry*, vol. 11, no. 15, pp. 1965–1982, 2004.

[7] K. N. Westlund, T. J. Krakower, S. W. Kwan et al., "Intracellular distribution of monoamine oxidase A in selected regions of rat and monkey brain and spinal cord," *Brain Research*, vol. 612, no. 12, pp. 221–230, 1993.

[8] P. Riederer and M. B. Youdim, "Monoamine oxidase activity and monoamine metabolism in brains of parkinsonian patients treated with l-deprenyl," *Journal of Neurochemistry*, vol. 46, no. 5, pp. 1359–1365, 1986.

[9] P. Riederer, W. Danielczyk, and E. Grünblatt, "Monoamine oxidase-B inhibition in Alzheimer's disease," *Neurotoxicology*, vol. 25, no. 1, pp. 271–277, 2004.

[10] M. García-Alloza, F. J. Gil-Bea, M. Díez-Ariza et al., "Cholinergic–serotonergic imbalance contributes to cognitive and behavioral symptoms in Alzheimer's disease," *Neuropsychologia*, vol. 43, no. 3, pp. 442–449, 2005.

[11] A. Benazzouz, T. Boraud, P. Dubedat et al., "Riluzole prevents MPTP-induced parkinsonism in the rhesus monkey: a pilot study," *European Journal of Pharmacology*, vol. 284, no. 3, pp. 299–307, 1995.

[12] W. E. Klunk, Y. Wang, G. F. Huang et al., "The binding of 2-(4′-methylaminophenyl)benzothiazole to postmortem brain homogenates is dominated by the amyloid component," *Journal of Neuroscience*, vol. 23, no. 6, pp. 2086–2092, 2003.

[13] P. Laurent, US Patent, 5, 719, 168, 1998.

[14] H. Reihlen, G. Hessling, W. Huhn et al., "Über aliphatische 1,2-Diamine," *Justus Liebigs Annalen der Chemie*, vol. 493, no. 1, p. 20, 1932.

[15] N. Ö. Can, D. Osmaniye, S. Levent et al., "Synthesis of new hydrazone derivatives for MAO enzymes inhibitory activity," *Molecules*, vol. 22, no. 8, p. 1381, 2017.

[16] B. Kaya Çavuşoğlu, B. N. Sağlık, Y. Özkay et al., "Design, synthesis, monoamine oxidase inhibition and docking studies of new dithiocarbamate derivatives bearing benzylamine moiety," *Bioorganic Chemistry*, vol. 76, pp. 177–187, 2018.

[17] B. N. Sağlık, S. Ilgın, and Y. Özkay, "Synthesis of new donepezil analogues and investigation of their effects on cholinesterase enzymes," *European Journal of Medicinal Chemistry*, vol. 124, pp. 1026–1040, 2016.

[18] Ü. Demir Özkay, Ö. D. Can, B. N. Sağlık et al., "Design, synthesis, and AChE inhibitory activity of new benzothiazole-piperazines," *Bioorganic and Medicinal Chemistry Letters*, vol. 26, no. 22, pp. 5387–5394, 2016.

[19] C. Binda, J. Wang, L. Pisani et al., "Structures of human monoamine oxidase b complexes with selective noncovalent inhibitors: safinamide and coumarin analogs," *Journal of Medicinal Chemistry*, vol. 50, no. 23, pp. 5848–5852, 2007.

[20] R. Granger, H. Orzalesi, and Y. Robbe, "Recherche d'agents radioprotecteurs-I. Diamines et dérivés apparentés a la phencyclidine," *Travaux de la Société de Pharmacie de Montpellier*, vol. 24, no. 1, pp. 244–255, 1964.

[21] G. Turan-Zitouni, A. Ozdemir, and Z. A. Kaplancikli, "Synthesis and antiviral activity of some (3,4-diaryl-3H-thiazo-2-ylidene)pyrimidine-2-yl amine derivatives," *Phosphorus, Sulfur, and Silicon and the Related Elements*, vol. 186, no. 2, pp. 233–239, 2011.

[22] N. V. Bhagavan, *Essentials of Medical Biochemistry: With Clinical Cases*, Elsevier, Burlington, MA, USA, 1st edition, 2011.

[23] International Organization for Standardization, *Biological Evaluation of Medical Devices-part 5: Tests for in Vitro Cytotoxicity ISO-10993-5*, International Organization for Standardization, 3rd edition, 2009.

[24] http://www.chem.ucla.edu/~harding/notes/strain_01.pdf, accessed 11.08.2016.